# Water-in-Supercritical CO2 Microemulsion for Synthesis of Carbon-Nanotube-Supported Pt Electrocatalyst for the Oxygen Reduction Reaction

**6 AUTHORS**, INCLUDING:

Kenichi Shimizu
University of Oxford
**17** PUBLICATIONS **311** CITATIONS

SEE PROFILE

I. Francis Cheng
University of Idaho
**83** PUBLICATIONS **1,804** CITATIONS

SEE PROFILE

Byunghoon Yoon
University of Colorado Boulder
**33** PUBLICATIONS **1,021** CITATIONS

SEE PROFILE

# Water-in-Supercritical CO$_2$ Microemulsion for Synthesis of Carbon-Nanotube-Supported Pt Electrocatalyst for the Oxygen Reduction Reaction

Kenichi Shimizu, I. Francis Cheng, Joanna S. Wang, Clive H. Yen, Byunghoon Yoon, and Chien M. Wai*

*Department of Chemistry, University of Idaho, Moscow, Idaho 83844-2343*

*Received January 23, 2008. Revised Manuscript Received April 11, 2008*

Four electrocatalysts, including a commercial Pt on carbon black (Pt-CB), were compared for performance in the reduction of oxygen. Three of the catalysts were prepared on the basis of the deposition of Pt onto carbon nanotubes using (i) water-in-supercritical CO$_2$ microemulsion (Pt-CNT SCME), (ii) direct supercritical CO$_2$ fluid deposition (Pt-CNT SC), and (iii) water-in-hexane microemulsion (Pt-CNT ME). Cyclic voltammetric studies yielded an electrochemically active surface area for Pt-CNT SCME at 31.1 m$^2$/g, which was the largest among all electrocatalysts tested in this work. Hydrodynamic polarization curves for oxygen reduction exhibited that the cell potential of the Pt-CNT SCME catalyst was over 350 mV more positive than the commercial Pt-CB system at 10 A/g of Pt. In chronoamperometric analyses, Pt-CNT SCME catalyst (6.6 × 10$^3$ A/g of Pt) generated 2.5 times more specific activity at 30 s than Pt-CNT ME (2.6 × 10$^3$ A/g of Pt) and 5 times more than the commercial Pt-CB (1.3 × 10$^3$ A/g of Pt). Tafel analysis indicated the exchange current density of 7.87 µA/cm$^2$ for Pt-CNT SCME that was significantly higher than the commercial Pt-CB (1.37 µA/cm$^2$).

## Introduction

Recent advancements in fuel cell technology have enabled small-scale fuel cells to be commercially available as an alternative energy source for small electronic devices.[1] Small-scale fuel cells, i.e., the proton-exchange membrane fuel cells (PEMFCs), are based on oxidation of hydrogen or lower aliphatic alcohols coupled with the reduction of oxygen to generate electricity. The reduction of oxygen in acidic medium can be expressed by the following reaction:

$$O_2 + 4H^+ + 4e^- \rightarrow 2H_2O \quad E^0 = 1.23 \text{ V vs NHE} \quad (1)$$

This reaction is the rate-limiting step for the overall process in hydrogen-fueled PEMFC.[2] Many efforts have been made to search for suitable and low-cost catalysts.[3–13] None, however, appear to have the performance of Pt for oxygen electroreduction. Accordingly, there is much interest in developing more efficient Pt-metal-based electrocatalysts.

Nanometer-sized particles have significantly increased the ratio of surface area/mass, resulting in the reduction of the applied Pt amount needed for an electrocatalysis.[14–16] An inert, high surface area and electrically conducting support, such as carbon black, allows for a dispersal of Pt nanoparticles with the cathode membrane of PEMFCs. Carbon nanotubes (CNTs) offer a similar approach and are reported to be a better support for the platinum nanoparticles than the conventional carbon black supports in PEMFC.[15,17] This is attributable to the high tensile strength, high resilience, and high electronic conductivity of CNTs.[18,19] CNT-supported Pt (Pt-CNT) catalysts have been prepared by a number of different methods, most of which involve the reduction of Pt$^{II}$ salts through means such as microemulsion,[15] chemical vapor deposition,[20] and electrochemical deposition.[21]

Pt-CNT prepared by a high-temperature microemulsion method in an ethylene glycol medium has been reported to

* To whom correspondence should be addressed. Telephone: (208) 855-6787. Fax: (208) 885-6173. E-mail: cwai@uidaho.edu.

(1) International Energy Agency. *Prospects for Hydrogen and Fuel Cells*; International Energy Agency: Paris, France, 2005.

(2) Gasteiger, H. A.; Kocha, S. S.; Sompalli, B.; Wagner, F. T. *App. Catal., B* **2005**, *56,* 9–35.

(3) Wang, B. *J. Power Sources* **2005**, *152,* 1–15.

(4) El-Deab, M. S.; Ohsaka, T. *Electrochim. Acta* **2002**, *47,* 4255–4261.

(5) Shao, M.-H.; Sasaki, K.; Adzic, R. R. *J. Am. Chem. Soc.* **2006**, *128,* 7408–7409.

(6) Fernández, J. L.; Raghuveer, V.; Manthiram, A.; Bard, A. J. *J. Am. Chem. Soc.* **2005**, *127,* 13100–13101.

(7) Ma, Z.-F.; Xie, X.-Y.; Ma, X.-X.; Zhang, D. Y.; Ren, Q.; Heâ-Mohr, N.; Schmidt, V. M. *Electrochem. Commun.* **2006**, *8,* 389–394.

(8) Gupta, S.; Tryk, D.; Zecevic, S. K.; Aldred, W.; Guo, D.; Savinell, R. F. *J. App. Electrochem.* **1998**, *28,* 673–682.

(9) Cheng, S.; Liu, H.; Logan, B. E. *Environ. Sci. Technol.* **2006**, *40,* 364–369.

(10) Yuasa, M.; Yamaguchi, A.; Oyaizu, K.; Fujito, Y.; Kitao, M.; Sato, T. *Polym. Adv. Technol.* **2005**, *16,* 702–705.

(11) Lefèvre, M.; Dodelet, J. P.; Berterand, P. *J. Phys. Chem. B* **2002**, *106,* 8705–8713.

(12) Convert, P.; Coutanceau, C.; Crour̈gneau, P.; GloaGuen, F.; Lamy, C. *J. Appl. Electrochem.* **2001**, *31,* 945–952.

(13) Zhao, F.; Harnisch, F.; Schröder, U.; Scholz, F.; Bogdanoff, P.; Herrmann, I. *Electrochem. Commun.* **2005**, *7,* 1405–1410.

(14) Pozio, A.; De Francesco, M.; Cemmi, A.; Cardellini, F.; Giorgi, L. *J. Power Source* **2002**, *105,* 13–19.

(15) Li, W.; Liang, C.; Zhou, W.; Qiu, J.; Zhou, Z.; Sun, G.; Xin, Q. *J. Phys. Chem. B* **2003**, *107,* 6292–6299.

(16) Higuchi, E.; Uchida, H.; Watanabe, M. *J. Electroanal. Chem.* **2005**, *583,* 69–76.

(17) Li, W.; Liang, C.; Qui, J.; Zhou, W.; Han, H.; Wei, Z.; Sun, G.; Xin, Q. *Carbon* **2002**, *40,* 791–794.

(18) Lu, J. P. *Phys. Rev. Lett.* **1997**, *79,* 1297–1300.

(19) Odom, T. W.; Huang, J.-L.; Kim, P.; Lieber, C. M. *J. Phys. Chem. B* **2000**, *104,* 2794–2809.

(20) Che, G.; Lakshmi, B. B.; Fisher, E. R.; Martin, C. R. *Nature* **1998**, *393,* 346–349.

(21) Premkumar, J.; Ramaraj, R. *J. Solid State Electrochem.* **1997**, *1,* 172–179.

be more active toward electro-reduction of oxygen compared to the conventional carbon-black-supported Pt catalyst prepared in the same manner.[15] The microemulsion method controls Pt particle size within a narrow size distribution by controlling the size of microemulsion that is determined by the molar ratio of water/surfactant known as the *W* value.[22–24] Our group has successfully modified the method so that the synthesis can take place at room temperature, i.e., eliminating the excessively high energy input.[25] Pt-CNT electrocatalysts synthesized by this modified method showed excellent nanometer-sized particle distributions. However, with all microemulsion methods, there is a possibility of leaving the surfactant residue on the catalyst, which could decrease its active surface area.[26–28]

In another approach, a solution of $Pt^{II}$(acetylacetonate)$_2$ in supercritical $CO_2$ fluid (sc$CO_2$) is subjected to reduction by $H_2$ in a moderately heated high-pressure reactor. The advantage of using sc$CO_2$ is that the solvent strength can easily be adjusted through the control of temperature and pressure, making it easier to control dissolution of active ingredients. Surfactant residues as well as dissolved reagents, such as acetylacetonate, can be effectively removed with sc$CO_2$ as the system is depressurized.[29] The use of sc$CO_2$ is considered to be within green chemistry practices because it is recyclable, nontoxic, and inexpensive.[30] Previous studies have shown that the direct sc$CO_2$ deposition method is capable of depositing Pt nanoparticles on the CNT surface with good electrocatalytic activity.[31–34] This method however lacks a mechanism for controlling the particle size of Pt. The combination of the method using sc$CO_2$ with microemulsion may allow for a better control of the particle sizes for Pt on CNT, while keeping the catalyst synthesis environmentally low impact. Several researchers have made use of the water-in-supercritical carbon dioxide microemulsion (SCME) to prepare nanoparticles.[35–38] However, to the best of our knowledge, no

study has prepared Pt-CNT using the SCME method for the purposes of the electrocatalysis of oxygen reduction.

## Experimental Section

**Chemicals and Materials.** Multiwalled carbon nanotubes (CNT, 60–100 nm in diameter, Nanostructured and Amorphous Materials, Inc., Los Alamos, NM) were purified by sonicating in 14 M $HNO_3$ for 1 h and then refluxed for 12 h in a mixture of concentrated $HNO_3$ and $H_2SO_4$, both of which were obtained from EMD Chemical, Inc. (ACS grade, Damstadt, Germany). $Pt^{II}$(acetylacetonate)$_2$ (97%) and sodium *bis*(2-ethylhexyl)sulfosuccinate (AOT, 99%) were purchased from Aldrich (Milwaukee, WI). Sodium tetrachloroplatanate ($Na_2Pt^{II}Cl_4$, 99.99%) was obtained from Alfa Aesar (Ward Hill, MA). High-purity hydrogen (>99%), carbon dioxide (99.99%), nitrogen (99.97%), and compressed air (19.5–23.5% $O_2$) were supplied by Oxarc (Spokane, WA).

The following chemicals and materials were used in the electrochemical characterization of Pt-CNTs. Sulfuric acid was titrated against tris(hydroxymethyl)amminomethane (Tris, Aldrich, St. Louis, MO) to obtain the exact concentration. Tris was dried in a desiccator overnight prior to the titration. A 5% Nafion 117 solution was obtained from Fluka (St. Gallen, Switzerland). Ethyl alcohol (200 proof, ACS/USP grade, Pharmco, Brockfield, CT) was used to dilute Nafion 117 solution. Purified water used in this study was prepared by passing the house distilled water through a Barnstead International cartridge (model D8922, Dubuque, IA). A 3.0 mm diameter glassy carbon working electrode and a Ag/AgCl (3 M NaCl) reference electrode were obtained from Bioanalytical Systems, Inc. (BASi, West Lafayette, IN). A glassy carbon rotating disk electrode (5.0 mm in diameter) was obtained from Pine Instrument Company (Grove City, PA). The counter electrode used in this study was a graphite rod purchased from Alfa Aesar (99%, Ward Hill, MA). Pt (9.5 wt %) on XC-72R surface-enhanced carbon black (abbreviated in this work as Pt-CB) was purchased from ETEK (Somerset, NJ) as a benchmark.

**Fabrication of Pt-CNT Direct Supercritical $CO_2$ Fluid Deposition (Pt-CNT SC).** A discussion of the direct sc$CO_2$ deposition method appears in previous papers [31,33] Therefore, an abbreviated version is mentioned in this report. Equal masses (20 mg) of CNT and $Pt^{II}$(acetylacetonate)$_2$ and a small amount of methanol were placed in a high-pressure reaction cell that was placed in an oven at 200 °C. $Pt^{II}$(acetylacetonate)$_2$ was dissolved/incubated into sc$CO_2$ by applying pressurized (120 bar) $CO_2$ into the reaction cell at 200 °C for 1 h. The $H_2/CO_2$ mixture was then introduced to the reaction cell, increasing the pressure to 160 bar. At that time, $Pt^{II}$ was reduced to metallic $Pt^0$ and deposited onto the CNT surface. The synthesized Pt-CNT SC was ultrasonically washed with methanol 5 times before use.

**Water-in-Hexane Microemulsion (Pt-CNT ME).** Synthesis of the water-in-hexane microemulsion as a template for depositing Pt nanoparticles on the surface of CNTs was reported previously by Yoon et al.[39,40] Acid-purified CNTs were added to the microemulsion solution of 0.1 M $Na_2PtCl_4$ and 0.02 M of a surfactant, AOT, in hexane at the *W* value of 12. The solution containing CNTs was continuously stirred and sonicated at room temperature for half an hour as $H_2$ gas was purged at 1 bar to reduce $Pt^{II}$ to $Pt^0$. Pt-CNT catalyst was allowed to settle once stirring was discontinued and was transferred to a glass vial. The vial was then centrifuged and decanted of excess solution. The AOT surfactant was recovered from the solution for reuse after the solution was carefully separated from Pt-CNT ME. The resultant Pt-CNT ME catalyst was rinsed with methanol several times before being air-dried.

**Water-in-Supercritical $CO_2$ Microemulsion (Pt-CNT SCME).** Microemulsion was prepared separately using hexane by the following procedure prior to the supercritical fluid synthesis. A total 98 $\mu$L of 0.1 M $Na_2PtCl_4$ solution, 15 mM of AOT (234 mg), 3 mL of hexane [8.5% (v/v, hexane/$CO_2$)], and 3–5 mg of

(22) Zhang, X.; Chan, K.-Y. *Chem. Mater.* **2003**, *15*, 451–459.

(23) Chan, K. Y.; Ding, J.; Ren, J.; Cheng, S.; Tsang, K. Y. *J. Mater. Chem.* **2004**, *14*, 505–516.

(24) López-Quintela, M. A.; Rivas, J. *J. Colloid Interface Sci.* **1993**, *158*, 446.

(25) Yoon, B.; Wai, C. M. Abstracts of papers, 231st ACS National Meeting, March 26–30, 2006, Atlanta, GA.

(26) Xiong, L.; Manthiram, A. *Electrochim. Acta* **2005**, *50*, 2323–2329.

(27) Solla-Gullón, J.; Montiel, V.; Aldaz, A.; Clavilier, J. *Electrochem. Commun.* **2002**, *4*, 716–721.

(28) Solla-Gullón, J.; Montiel, V.; Aldaz, A.; Clavilier, J. *J. Electroanal. Chem.* **2000**, *491*, 69–77.

(29) Cansell, F.; Chevalier, B.; Demourgues, A.; Etourneau, J.; Even, C.; Garrabos, Y.; Pessey, V.; Petit, S.; Tressaud, A.; Weill, F. *J. Mater. Chem.* **1999**, *9*, 67–75.

(30) DeSimone, J. M. *Science* **2002**, *297*, 799–803.

(31) Ye, X.-R.; Lin, Y.; Wang, C.; Engelhard, M. H.; Wang, Y.; Wai, C. M. *J. Mater. Chem.* **2004**, *14*, 908–913.

(32) Lin, Y.; Cui, X.; Yen, C.; Wai, C. M. *J. Phys. Chem. B* **2005**, *109*, 14410–14415.

(33) Yen, C. H.; Cui, X.; Pan, H.-B.; Wang, S.; Lin, Y.; Wai, C. M. *J. Nanosci. Nanotechnol.* **2005**, *5*, 1852–4857.

(34) Yen, C. H.; Shimizu, K.; Lin, Y.-Y.; Bailey, F.; Cheng, I. F.; Wai, C. M. *Energy Fuels* **2007**, *21*, 2268–2271.

(35) Ohde, H.; Hunt, F.; Wai, C. M. *Chem. Mater.* **2001**, *13*, 4130–4135.

(36) Ohde, M.; Ohde, H.; Wai, C. M. *Chem. Commun.* **2002**, 2388–2389.

(37) Liu, J.; Raveendran, P.; Shervani, Z.; Ikushima, Y. Synthesis of Ag2S quantum dots in water-in-$CO_2$ micremulsions. *Chem. Commun.* **2004**, 2582–2583.

(38) Liu, J.; Raveendran, P.; Shervani, Z.; Ikushima, Y.; Hakuta, Y. *Chem.–Eur. J.* **2005**, *11*, 1854–1860.

(39) Yoon, B.; Kim, H.; Wai, C. M. *Chem. Commun.* **2003**, 1040–1041.

(40) Yoon, B.; Wai, C. M. *J. Am. Chem. Soc.* **2005**, *127*, 17174–17175.

**Scheme 1. Schematic Diagram of Water-in-Supercritical CO₂ Microemulsion Synthesis**
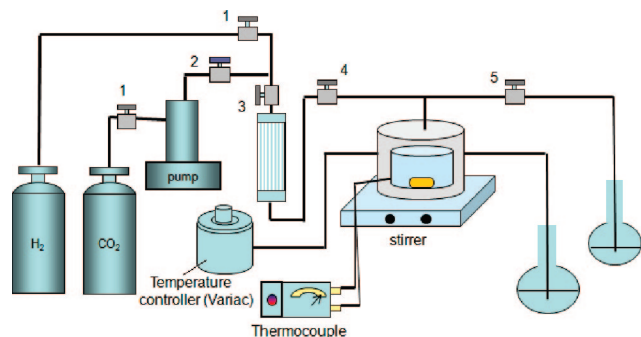


purified CNTs were added to a glass vial ($W = 10$). A magnetic stirrer was used to agitate the mixture for 20 min. A small amount of hexane is necessary to increase the solubility of the AOT surfactant, which is otherwise insoluble in scCO₂.

Synthesis using water-in-scCO₂ microemulsion was carried out in the following manner: The apparatus for this synthesis was set up as shown in Scheme 1. A small glass vial, containing the microemulsion, was placed into a stainless-steel extraction vessel (35.3 mL internal volume), and CO₂ was introduced in the reactor with a syringe pump (Isco, model 260D, Lincoln, NE). The pressure of the vessel was kept at 190 bar for 1.5 h prior to the addition of a reducing agent. A mixture of CO₂ and H₂ (12 bar) at a total pressure of 230 bar was then charged into the reactor for reduction of Pt. The final pressure of the system was adjusted to 250 bar by applying CO₂, while the scCO₂ flow rate was controlled by the outlet high-pressure valve. At the oven exit, stainless-steel tubing (316 SS, ¹/₁₆ in external diameter and 0.030 in internal diameter) with a length of 20 cm was used as the pressure restrictor for CO₂. The reactor was loaded on the bottom of the thermal mantle, which was connected to a thermal voltage controller, and was wrapped with a glass-wool insulator (not shown in Scheme 1). The synthesis was conducted at 40 °C, and temperature of the high-pressure cell was monitored using a thermocouple. The solution in the reactor was agitated with a magnetic stirrer for 1 h followed by 0.5 h dynamic flushing. This dynamic flush was undertaken by flushing with pressure of 250 bar with 12 bar H₂ at a flow rate of 0.1–0.2 mL/min. The system was then slowly depressurized with the same flow rate. The Pt-CNT SCME was washed with methanol and isolated using centrifugation followed by oven drying at 80 °C.

**Transmission Electron Microscopy (TEM) Image and X-ray Diffraction (XRD).** The TEM micrograph of Pt-CNT SCME was taken with JEOL JEM 2010-1200EXII at an operating voltage of 100 keV. TEM images for all other catalysts were taken at the operating voltage 200 keV. Energy dispersive X-ray spectroscopy (EDS) was used to obtain Pt composition of Pt-CNT SCME. Sample dispersed in methanol was directly placed on an aluminum support and dried in ambient conditions before analyzed in Zeiss Supra 55 FESEM at 20 kV. According to the spectrum, the weight percent of Pt in the sample is 17.7% in Pt-CNT SCME. EDS was also applied on Pt-CNT ME and Pt-CNT SC using Armray 5500 at 20 kV and revealed 16.8 wt % Pt and 16 wt % Pt, respectively. XRD patterns were obtained using a Siemens diffractometer D5000. The region of the diffraction angle, $2\theta$, between 10° and 90° was analyzed at a step size of 0.02°/s. The slow step size revealed the small peak, which otherwise could be buried in the noise.

**Preparation of Electrode and Electrochemical Analysis.** Electrodes were modified according to the following steps. The glassy carbon working electrode was polished with aqueous slurry of 1 μm alumina (Pace Tech., Tucson, AZ) on polishing cloth (Mark V Laboratory, East Granby, CT). The electrode was then briefly sonicated to remove the alumina residues from the electrode surface. Nafion 117 was prepared by diluting the commercial 5% solution with a 50/50 (v/v) mixture of water/ethanol. Electrocatalysts were mixed with the Nafion solution to make a 1 mg/mL catalyst/Nafion mixture. To ensure that electrocatalysts were evenly suspended,

the mixture was sonicated for 30 min prior to each electrode modification. A 10 μL aliquot of the mixture of Pt-CNT catalysts and a 13 μL aliquot of the mixture of Pt-CB were dispensed by micropipette onto the surface of the electrode followed by 2 h of drying at room temperature in the ambient atmosphere. The different amounts of catalyst mixture were applied to keep the platinum content close to each other.

Cyclic voltammograms (CVs) were collected on a BASi CV-50W potentiostat (version 2.31, West Lafayette, IN). Hydrodynamic measurements were carried out using a single-element rotator (AFCPRB, Pine Instrument Co., Grove City, PA) on BASi CV-50W potentiostat. Tafel analysis was conducted with the rotating disk electrode on a Gamry Instrument PC4 PC-based potentiostat for DC corrosion measurement (Framework version 4.3, Warminster, PA), and Tafel curves were analyzed using Gamry Echem Analyst software programs (version 1.30). All voltammetric analyses were conducted by making use of a conventional three-electrode cell consisting of a Ag/AgCl reference electrode (3 M NaCl), a carbon rod auxiliary electrode, and a modified glassy carbon working electrode in 1.0 M H₂SO₄ solution. The solution was purged with nitrogen for at least 30 min to deoxygenate for background collection and then purged with air for at least 30 min to collect the oxygen reduction scans. Potentials reported in this paper are all referred to the Ag/AgCl reference electrode unless otherwise noted. In cyclic voltammetric experiments, potential was scanned at 50 mV/s between 900 and 0 mV for the oxygen reduction reaction. In addition, potential was swept between 1000 and −220 mV only in deoxygenated sulfuric acid solution to obtain the hydrogen adsorption/desorption. For hydrodynamic voltammetry, potential was scanned at 10 mV/s from 900 to 0 mV. In chronoamperometry, potential was stepped from 850 to 600 mV, and then the potential was kept for 30 s, while the electrode was rotated at 2000 rpm. Finally, the Tafel analysis was conducted by scanning from −100 to 1000 mV at 1 mV/s, while the electrode was rotated at 500 rpm.

## Results and Discussion

The TEM micrograph in Figure 1 displays the electrocatalysts used in this work. Pt-CNT SCME shown in Figure 1a displayed a pattern of well-dispersed platinum nanoparticles on the CNT surface. The particle dispersion observed in the figure is very comparable to that in Figure 1b, i.e., Pt-CNT ME. This indicates that the water-in-scCO₂ microemulsion is as effective system on depositing Pt nanoparticles onto CNT as water-in-oil microemulsion. Because of the resolution of the TEM image, it was not possible to measure the particle diameters accurately or precisely. Therefore, average particle diameters of Pt on CNT were characterized using powder XRD.

Figure 2 shows the characteristic XRD pattern of the Pt-CNT SCME catalyst with Pt peak positions consistent with observations made by a number of previous researchers.[15,26,41] A diffraction peak at ca. 25° shows the (002) diffraction pattern, which is typical of graphite.[15] The sharpness of the carbon support peaks in Figure 2 is attributed to the hexagonal structure of the CNT support. On the other hand, the broad peak within the insert of Figure 2 corresponds to the less defined crystal structure of the carbon black support from the commercial catalyst.[15] The peak at 40° is the (111) diffraction pattern of platinum nanoparticles. Furthermore, Pt peaks of (200), (220), (311), and (222), which appear at the diffraction degrees of 46°, 68°, 81°, and 86°, respectively, indicate that Pt nanoparticles have a face center cubic crystal structure.[15,42] The mean particle

(41) Xiong, L.; Kannan, A. M.; Manthiram, A. *Electrochem. Commun.* **2002**, *4*, 898–903.

(42) Lafuente, E.; Muñoz, E.; Benito, A. M.; Maser, W. K.; Martínez, M. T.; Alcaide, F.; Ganborena, L.; Cendoya, I.; Miguel, O.; Rodríguez, J.; Urriolebeitia, E. P.; Navarro, R. *J. Mater. Res.* **2006**, *21*, 2841–2846.
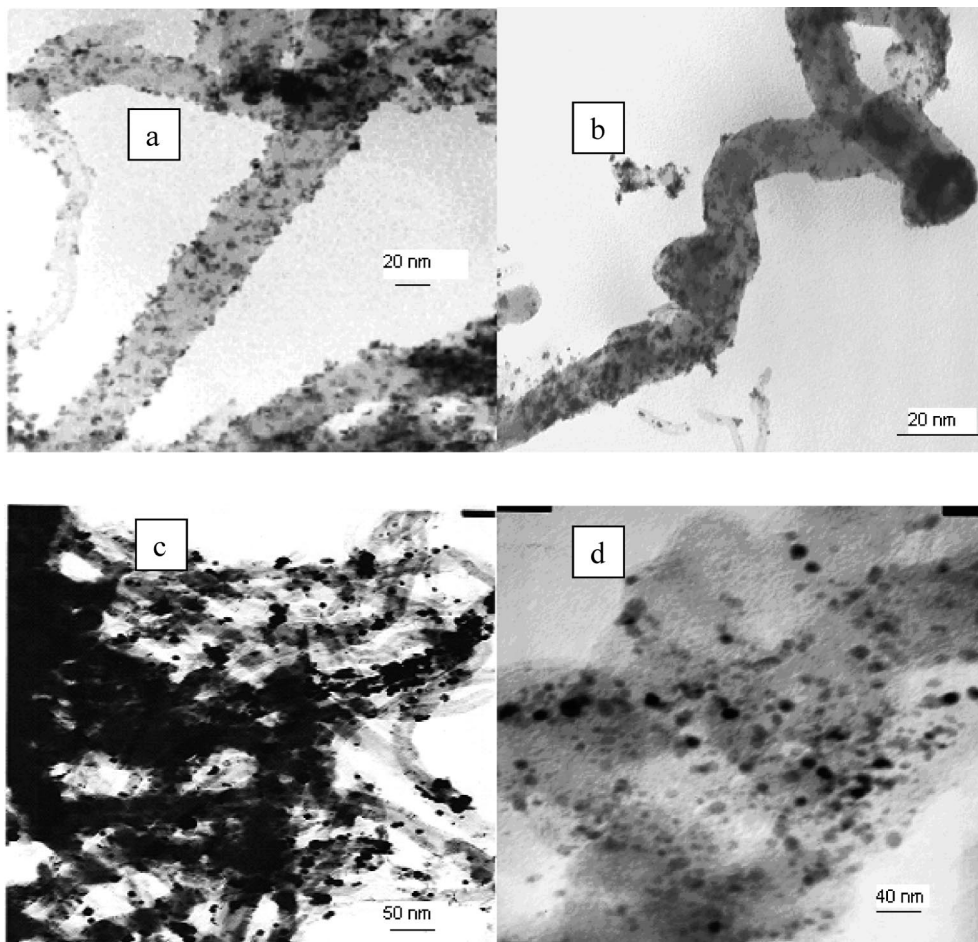
**Figure 1.** TEM images of (a) Pt-CNT synthesize by water-in-supercritcal $CO_2$ microemulsion (SCME), (b) Pt-CNT water-in-oil microemulsions (ME), (c) Pt-CNT direct-supercritical $CO_2$ deposition (SC), and (d) commercial Pt-CB (carbon black).
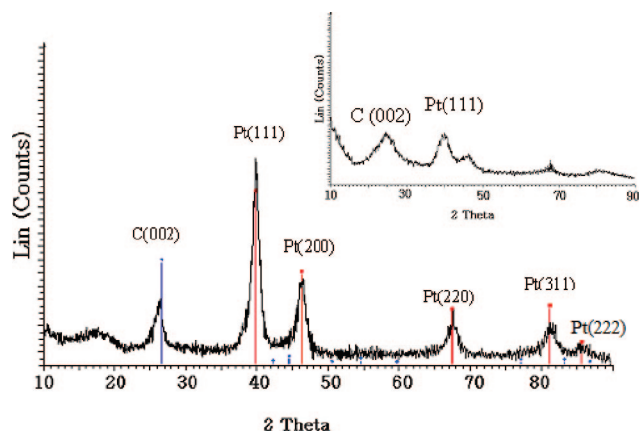


**Figure 2.** XRD pattern of Pt-CNT SCME. Numbers in the parentheses are the Miller indices, indicating the diffraction surface of platinum (Pt) and graphite (C). The inset shows the XRD pattern of the commercial catalysts (PtCB). The average particle diameter (8.7 nm) is estimated from the peak for Pt(220) using eq 2.

size of Pt on the CNT support was estimated from the (220) diffraction peak using Scherrer's formula shown below.[15]

$$L = \frac{0.94 \lambda_{\kappa\alpha t}}{B_{(2\theta)} \cos \theta} \quad (2)$$

In the above equation, $L$ represents the average particle diameter, $\lambda_{\kappa\alpha t}$ represents the wavelength of X-ray radiation (Cu K$\alpha$ source, $\lambda = 0.154\ 18$ nm), $B_{2\theta}$ represents the full width at the half-height in radians of a diffraction peak of the (220) crystal

structure, and $\theta$ represents the diffraction angle of the peak. The calculated Pt particle size in Pt-CNT SCME was 8.7 nm, which was within the range for Pt-CNT SC that was reported in a previous paper,[32] i.e., 5−10 nm.

**Catalyst Characterization with Cyclic Voltammetry.** Electroactive surface areas were estimated using cyclic voltammetry in 1.0 M $H_2SO_4$ under nitrogen-purged conditions at a potential sweep rate of 50 mV/s. Figure 3a shows hydrogen adsorption/desorption waves on the Pt-CNT SCME modified electrode. The CV was limited to a cathodic threshold of −220 mV, because beyond that potential, reduction of water became significant. The formation of the gaseous product was detrimental to the catalyst/Nafion layer to slough off from the glassy carbon electrode. Moreover, vigorous gas formation severely damaged the surface of the working electrode by etching glassy carbon material. The electroactive surface area was estimated from the hydrogen desorption curve, which is indicated as a shaded area in Figure 3a. This area was integrated using the analysis program packaged with the BAS CV-50w potentiostat, which is calculated by the following equation:[43]

$$S = \frac{A}{v \cdot 2.10 \times 10^{-4}\ \text{C/cm}^2} \quad (3)$$

where $S$ is the electroactive surface area (cm$^2$), $A$ is the area under the current−potential curve (ampere volts), $v$ is the sweep rate (0.05 V/s), and $2.10 \times 10^{-4}$ C/cm$^2$ is the average charge associated with adsorption/desorption of the hydrogen mono-

(43) Biegler, T.; Rand, D. A. J.; Woods, R. *J. Electroanal. Chem.* **1971**, *29*, 269–277.
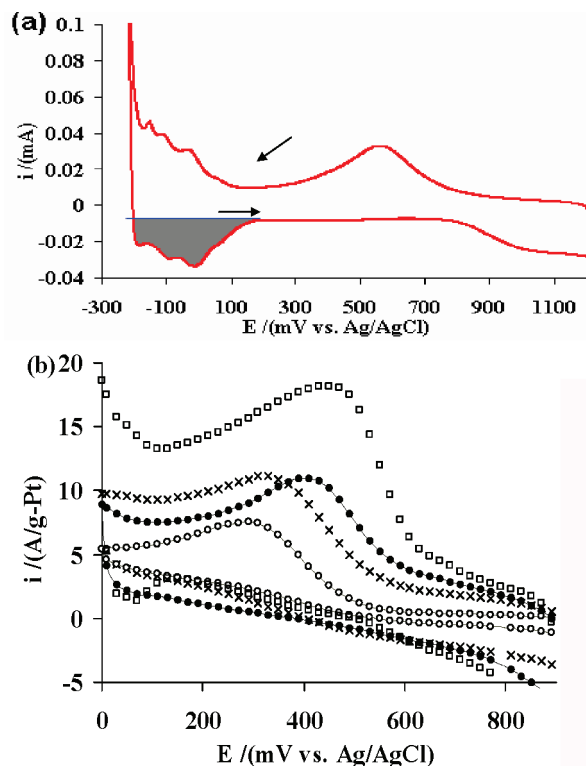
**Figure 3.** (a) Cyclic voltammogram on Pt-CNT SCME in nitrogen-purged 1.0 M H$_2$SO$_4$. The shaded area was used to calculate the electroactive surface area of platinum nanoparticles. (b) Cyclic voltammograms of the oxygen reduction on the electrode modified by Pt-CNT SCME (□), Pt-CNT ME (●), Pt-CNT SC (×), and commercial PtCB (○) in air-purged 1.0 M H$_2$SO$_4$. The scan rate was at 50 mV/s.

**Table 1. Peak Potentials and Peak Currents for the Electro-reduction of Oxygen Based on Eq 1[a]**

|  | $E_p$ (mV) | $i_p$ (A/g of Pt) | surface area (m$^2$/g of Pt) |
|---|---|---|---|
| commercial Pt-CB | 288 | 6.86 | 9.15 (±4.74) |
| Pt-CNT SCME | 499 (±35) | 11.5 (±1.8) | 31.1 (±3.4) |
| Pt-CNT ME | 421 (±8) | 5.47 (±0.24) | 9.46 (±2.59) |
| Pt-CNT SC | 334 (±14) | 7.25 (±0.18) | 6.04 (±1.09) |

[a] Numbers in the parentheses represents one standard deviation unit.

layer on the platinum surface.[28,43–46] The largest electroactive surface area per gram of platinum was achieved by Pt-CNT SCME at 31.1 m$^2$/g Pt. This observation suggests that the surfactant used during the synthesis was more effectively removed by using sc-CO$_2$ as a cosolvent. This surface area was over 3 times larger than the other catalysts tested, including the commercial Pt-CB (Table 1).

Figure 3b shows CVs of the catalytic electro-reduction of dissolved oxygen. Peak potentials and currents are summarized in Table 1. In the figure, the current is reported as mass activity (A/g of Pt) to illustrate the relative activities of each electrocatalyst. Larger capacitive currents observed with Pt-CNT electrocatalysts indicate greater surface area of the substrate in comparison to carbon-black-based systems. Pt-CNT SCME demonstrated the highest mass activity (11.5 A/g of Pt) toward oxygen reduction reaction in comparison to the other catalysts;

(44) Pinheiro, A. L. N.; Oliveira-Neto, A.; de Souza, E. C.; Perez, J.; Paganin, V. A.; Ticianelli, E. A.; Gonzales, E. R. *J. New. Mat. Electrochem. Syst.* **2003**, *6*, 1–8.

(45) Lakshminarayanan, V.; Srinivasan, R.; Chu, D.; Gilman, S. *Surf. Sci.* **1997**, *392*, 44–51.

(46) Paulus, U. A.; Wokaun, A.; Scherer, G. G.; Schmidt, T. J.; Stamenkovic, V.; Radmilvoic, V.; Markovic, N. M.; Ross, P. N. *J. Phys. Chem. B* **2002**, *106*, 4181–4191.
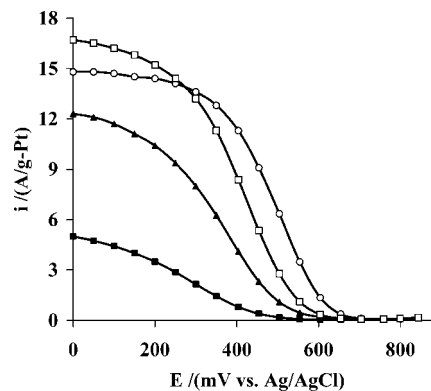


**Figure 4.** Comparison of the polarization curve for O$_2$ reduction on Pt-CNT SCME (○), Pt-CNT ME (□), commercial PtCB (▲), and Pt-CNT SC (■) in 1.0 M H$_2$SO$_4$ solution saturated with air. The scan rate was at 10 mV/s, and the rotation speed was at 2000 rpm. The current is expressed as A/g of Pt. The background was subtracted from each voltammogram.
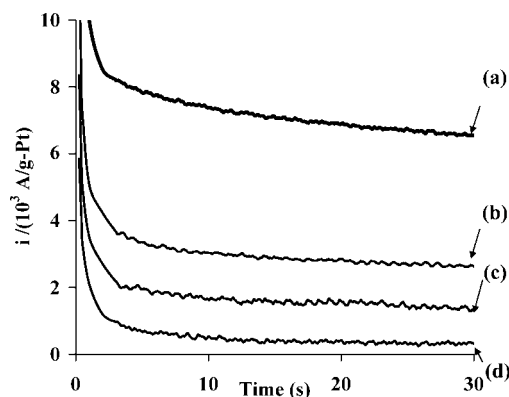


**Figure 5.** Chronoamperometric curve for O$_2$ reduction on (a) Pt-CNT SCME, (b) Pt-CNT ME, (c) Pt-CB, and (d) Pt-CNT SC in 1.0 M H$_2$SO$_4$ solution saturated with air.

in addition to that, the observed peak potential was near 500 mV, which is 200 mV more positive than the commercial catalyst (Table 1). The Pt-CB electrocatalyst was 6.86 A/g of Pt, which is similar to other investigations.[47] Furthermore, the onset potential of the Pt-CNT SCME catalyst was as low as 700 mV, which is very close to the cell-operating potential of the direct methanol fuel cells.

**Hydrodynamic Voltammetric Analysis.** The kinetic limitation of oxygen reduction is an important issue in the fuel cell system because it lowers the potential output by as much as 300 mV from the thermodynamically estimated cell potential.[48] Figure 4 shows hydrodynamic polarization curves for the electrocatalyst on the oxygen reduction reaction obtained using a rotating disk electrode at 2000 rpm. This curve of Pt-CNT SCME shows that there was a shift of over +100 mV when compared to the commercial Pt-CB at 1 A/g of Pt. Moreover, at 10 A/g of Pt, the potential difference reached its maximum at 350 mV. This is a clear indication of enhanced catalytic activity of Pt-CNT SCME over the commercial Pt-CB. Figure 5 illustrates a chronoamperometric analysis at 600 mV. The mass activity of Pt-CNT SCME obtained from Figure 5 at 30 s was 6.6 × 10$^3$ A/g of Pt. This value was 5 times higher than the commercial catalyst (1.3 × 10$^3$ A/g of Pt) and 2.5 times higher than the Pt-CNT ME (2.6 × 10$^3$ A/g of Pt). The superior

(47) Maye, M. M.; Kariuki, N. N.; Luo, J.; Han, L.; Njoki, P.; Wang, L.; Lin, Y.; Naslund, R.; Zhoug, C.-J. *Gold Bull.* **2004**, *37*, 217–223.

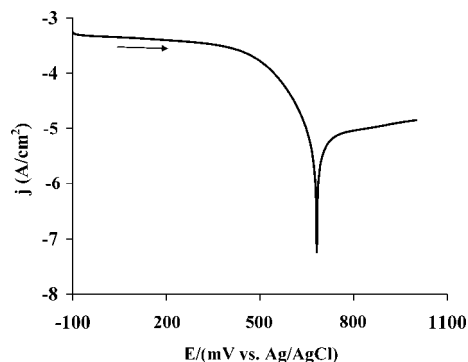(48) Ralph, T. R.; Hogarth, M. P. *Platinum Metals Rev.* **2002**, *46*, 3–14.

**Figure 6.** Tafel curve for $O_2$ reduction on Pt-CNT SCME in air-saturated 1 M $H_2SO_4$. The scan was collected at 1 mV/s, while electrode was rotated at 500 rpm. The arrow shows the direction of the scan. Exchange current densities are presented in Table 2.

catalytic activity of Pt-CNT SCME is attributable to the large active surface area as measured from CV.[49]

Hydrodynamic voltammetric analyses were conducted to estimate the number of electrons transferred per $O_2$ in air-saturated 1.0 M $H_2SO_4$. Complete consumption of $O_2$ is indicated by a four electron transfer as shown in eq 1. The current densities in the hydrodynamic voltammogram are composed of the diffusion-limited current, $i_d$, and the kinetically limited current, $i_K$. The diffusion limited current, $i_d$, varies with the rotation speed of the electrode and is defined in the following Levich equation:[50]

$$i_d = 0.62 n F A D^{2/3} \omega^{1/2} \nu^{-1/6} C^b \quad (4)$$

where $n$ is the number of electrons involved in the oxygen reduction reaction, $F$ is Faraday's constant, $A$ is the geometric surface area of the disk electrode (0.192 cm$^2$), $D$ is the diffusion coefficient of oxygen in aqueous solution ($1.93 \times 10^{-5}$ cm$^2$/s),[4] $\omega$ is the angular velocity in revolutions per second, $\nu$ is the kinematic viscosity of water ($9.5 \times 10^{-3}$ cm$^2$/s),[4] and $C^b$ is the bulk concentration of dissolved oxygen ($2.67 \times 10^{-7}$ mol/cm$^3$). The Levich plot ($1/i$ versus $1/\omega^{1/2}$) exhibited a linear diagram, which held with a nonzero intercept. This is because of the kinetically limited current that is independent of the rotation speed of the rotating disk electrode. The kinetically limited current consists of the mass transport of oxygen within the thin catalyst layer on the electrode surface as well as the charge-transfer process.[46] The slope of the linear plot revealed the number of electrons transferred, $n$, as is indicated in eq 4. The value of $n$ observed with the Pt-CNT SCME was 3.7 electrons in comparison to 3.4, 3.1, and 2.9 electrons observed from Pt-CNT SC, the commercial Pt-CB, and Pt-CNT ME, respectively. Pt-CNT SCME was clearly the most efficient in terms of complete consumption of oxygen.

**Tafel Analysis.** To gain a better understanding of the kinetic parameters in the oxygen reduction reaction, Tafel analyses were conducted on disk electrodes modified with the four catalytic system of this study (Figure 6). The rotation rate was held at 500 rpm to ensure a significant and constant mass transfer of dissolved oxygen to the surface of the modified electrode. Figure 6 shows a Tafel curve of Pt-CNT SCME, which was scanned in the anodic direction in air-saturated 1.0 M $H_2SO_4$, and Table 2 summarizes the values generated for all electrocatalysts. The

**Table 2. Anodic Tafel Plot Was Scanned at 1 mV/s with a Rotating Disk Electrode Rotated at 500 rpm for the Reduction of Oxygen, Eq 1**[a]

|  | Tafel slope (mV/decade) | $j_0$ ($\mu$A/cm$^2$) | $E_{eq}$ (mV$_{Ag/AgCl}$) |
| --- | --- | --- | --- |
| commercial Pt-CB | 126 ($\pm$8) | 1.37 ($\pm$0.93) | 617 ($\pm$48) |
| Pt-CNT SCME | 112 ($\pm$15) | 7.87 ($\pm$2.89) | 668 ($\pm$25) |
| Pt-CNT ME | 126 ($\pm$25) | 4.30 ($\pm$1.54) | 622 ($\pm$55) |
| Pt-CNT SC | 140 ($\pm$13) | 1.51 ($\pm$0.46) | 569 ($\pm$21) |

[a] Reaction cells contained 1.0 M $H_2SO_4$ purged with air for more than half an hour. Exchange current densities, $j_0$, are given as $\mu$A per geometric area (cm$^2$) of the electrode. Equilibrium potentials, $E_{eq}$, found where $\eta = 0$, have the given unit of mV versus Ag/AgCl.

Tafel analysis must be carried out scanning in the anodic direction, i.e., from negative to positive, because a cathodic direction would be obscured by the reduction of surface oxides as shown in eq 5.

$$PtO + 2H^+ + 2e^- \rightarrow Pt + H_2O \quad E^0 = 0.98 \text{ V vs NHE} \quad (5)$$
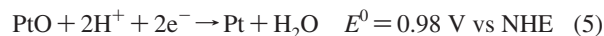
Tafel slopes for the oxygen reduction reaction catalyzed by carbon-supported platinum and nonsupported platinum catalysts have been reported by a number of researchers, and Tafel slopes can be generalized to two groups: ca. 120 mV/decade[44,46,51–53] and ca. 60 mV/decade.[26,44,46,52,54–56] Generally, the latter value is observed when the charge transfer is the rate-limiting step for the oxygen reduction reaction.[57] The Tafel slope of ca. 120 mV/decade attributes the rate-determining process to the transport of oxygen to the electrocatalyst.[58] The results summarized in Table 2 indicate that the mass transport of oxygen is the rate-limiting process. In addition, the difference of the Tafel slopes among the electrocatalysts is small, indicating that the reaction mechanism is the same for all electrocatalysts tested in this study.[59] Pt-CNT SCME exhibited a significantly large anodic exchange current density of 7.87 $\mu$A/cm$^2$ in comparison to 1.37 $\mu$A/cm$^2$ of the commercial catalyst. This result indicates that the oxygen reduction reaction on Pt-CNT SCME holds the fastest rate of the reaction at equilibrium; thus, it shows the best catalytic characteristic among the four systems examined in this work.

**Conclusion**

In this study, we prepared three Pt-CNT electrocatalysts for the reduction of oxygen in fuel cells. The mass activity of the Pt-CNT SCME system was found to be the highest (Table 1) at 11.5 A/g of Pt, which was about 1.7 times higher than the commercial reference system based on carbon black. Furthermore, the hydrodynamic polarization curve showed a significant potential shift of +350 mV for Pt-CNT SCME at 10 A/g of Pt

(49) Tang, H.; Chen, J. H.; Huang, Z. P.; Wang, D. Z.; Ren, Z. F.; Nie, L. H.; Kuang, Y. F.; Yao, S. Z. *Carbon* **2004**, *42*, 191–197.

(50) Bard, A. J.; Faulkner, L. R. *Electrochemical Methods Fundamentals and Applications*, 2nd ed.; John Wiley and Sons, Inc.: New York, 2001; p 339.

(51) Wang, J. X.; Markovic, N. M.; Adzic, R. R. *J. Phys. Chem. B* **2004**, *108*, 4127–4133.

(52) Wakabayashi, N.; Takechi, M.; Uchida, H.; Watanabe, M. *J. Phys. Chem. B* **2005**, *109*, 5836–5841.

(53) Maruyama, J.; Abe, I. *J. Electroanal. Chem.* **2003**, *545*, 109–115.

(54) Gnanamuthu, D. S.; Petrocelli, J. V. *J. Electrochem. Soc.* **1967**, *114*, 1036–1041.

(55) Girishkumar, G.; Vinodgopal, K.; Kamat, P. V. *J. Phys. Chem. B* **2004**, *108*, 19960–19966.

(56) Yang, H.; Vogel, W.; Lamy, C.; Alonso-Vante, N. *J. Phys. Chem. B* **2004**, *108*, 11024–11034.

(57) The Tafel slope can be estimated with the following equation:

$$\text{Tafel slope} = nRT/\alpha F$$

Thus, because the rate-determining step is the charge transfer ($n = 1$) and assuming $\alpha = 0.5$, the Tafel slope is estimated to be 60 mV/decade.

(58) Paganin, V. A.; Oliveira, C. L. F.; Ticianelli, E. A.; Springer, T. E.; Gonzales, E. R. *Electrochim. Acta* **1998**, *43*, 3761–3766.

(59) Meng, H.; Shen, P. K. *J. Phys. Chem. B* **2005**, *109*, 22705–22709.

when compared to the commercial Pt-CB, indicating the possibility for a significant increase in power output for a fuel cell based on our catalyst. The same analysis indicated a more complete consumption of oxygen (3.7 $e^-$ per $O_2$) for the newly synthesized Pt-CNT SCME over commercial Pt-CB (3.1 $e^-$ per $O_2$).

EF800052B